International Journal for Modern Trends in Science and Technology
Volume 11, Issue 05, pages 1209-1223
ISSN: 2455-3778 online
Available online at: http://www.ijmtst.com/vol11issue05.html
DOI: https://doi.org/10.5281/zenodo.15511414

Hybrid AC Microgrid using Solar, Wind, Battery, and Diesel Generator Integration for Enhanced Power Quality, Load Balancing, and Reduced Fuel Consumption

A.D. Deepa[1], M Harish[2], Dr. K. Siva Kumar [3]

[1]PG Student, Dept. of Electrical & Electronics Engineering, Sri Venkatesa Perumal College of Engineering and Technology, Puttur, Andhra Pradesh, India
[2]Assistant Professor, Dept. of Electrical & Electronics Engineering, Sri Venkatesa Perumal College of Engineering and Technology, Puttur, Andhra Pradesh, India
[3]Professor, Dept. of Electrical & Electronics Engineering, Sri Venkatesa Perumal College of Engineering and Technology, Puttur, Andhra Pradesh, India

To Cite this Article
A.D. Deepa, M Harish & Dr. K. Siva Kumar (2025). Hybrid AC Microgrid using Solar, Wind, Battery, and Diesel Generator Integration for Enhanced Power Quality, Load Balancing, and Reduced Fuel Consumption. International Journal for Modern Trends in Science and Technology, 11(05), 1209-1223. https://doi.org/10.5281/zenodo.15511414

Article Info
Received: 27 April 2025; Accepted: 22 May 2025.; Published: 25 May 2025.

KEYWORDS

Hybrid AC Microgrid, Solar Photovoltaic (PV), Wind Energy, Battery Energy Storage System (BESS), Diesel Generator, Maximum Power Point Tracking (MPPT), Bidirectional DC-DC Converter, Power Quality, Frequency Stability, Load Balancing

ABSTRACT

This paper presents a hybrid renewable energy-based AC microgrid system integrating a diesel generator, solar photovoltaic (PV), wind turbine, and battery energy storage to enhance power quality, frequency stability, and power management efficiency. The proposed system aims to reduce the high operational cost associated with diesel generators by prioritizing renewable energy sources and utilizing a battery backup. Due to the intermittent nature of solar and wind energy, a DC–DC bidirectional buck–boost converter manages the battery storage, ensuring continuous power supply and effective load balancing during variable generation periods. The solar PV system is interfaced through a boost converter employing a Perturb and Observe (P&O) Maximum Power Point Tracking (MPPT) algorithm, while wind energy conversion uses a Permanent Magnet Synchronous Generator (PMSG) with an MPPT-controlled AC–DC converter. To maintain superior power quality and frequency regulation within the microgrid, a cascaded Generalized Second-Order Integrator (C-SOGI)-based Phase-Locked Loop (PLL) is implemented in the control scheme. With reduced dependence on the diesel generator, the system significantly

lowers fuel consumption and emissions, contributing to both economic and environmental benefits. MATLAB/Simulink-based simulation results demonstrate that the proposed approach improves overall system performance by reducing total harmonic distortion, enhancing dynamic response, and ensuring stable, cost-effective, and resilient operation under varying load and generation conditions.

1. Introduction

In recent decades, the rapid depletion of fossil fuel resources along with increasing environmental concerns has accelerated the global shift towards sustainable and renewable energy systems. Conventional power generation, which relies primarily on coal, oil, and natural gas, has contributed significantly to greenhouse gas emissions, air pollution, and climate change. These issues have driven an urgent need for cleaner and more sustainable alternatives [1], [2]. In this context, hybrid microgrids have emerged as a promising solution for providing reliable, affordable, and environmentally friendly electricity. Hybrid microgrids are small-scale, localized power systems that integrate renewable energy sources, energy storage, and conventional generators to deliver stable power supply [3], [4]. Hybrid microgrids can operate both in grid-connected mode and in islanded mode, thereby enhancing reliability, improving power quality, and increasing resilience against grid disturbances and outages [5]. A typical hybrid microgrid system integrates solar photovoltaic (PV) panels, wind turbines, battery energy storage systems (BESS), and diesel generators, leveraging the strengths of each power source and compensating for their limitations [6]. Diesel generators are commonly used in remote and off-grid applications due to their ability to provide stable and controllable power output. However, diesel generators depend on fossil fuels, which results in high operating costs, noise pollution, and the emission of harmful gases such as carbon dioxide, nitrogen oxides, and particulate matter. These emissions have a negative impact on the environment and public health [7], [8]. Therefore, reducing diesel generator usage by increasing the share of renewable energy sources is a key objective in the design of modern microgrids. Renewable energy sources such as solar PV and wind power are abundant and environmentally friendly. However, they are inherently intermittent and stochastic due to their dependence on weather conditions, which causes significant challenges in maintaining continuous power supply, system stability, and power quality within the microgrid [9], [10]. Solar PV output fluctuates with changes in solar irradiance and temperature, while wind power varies depending on wind speed and turbulence [11], [12]. These fluctuations can cause voltage and frequency deviations as well as increased total harmonic distortion, which may damage sensitive electrical equipment if not managed properly [13]. To address these challenges, battery energy storage systems are widely deployed in hybrid microgrids to provide services such as load leveling, peak shaving, frequency regulation, and backup power during outages [14], [15]. Batteries help smooth the variability of renewable energy by storing excess power generated during periods of high renewable output and supplying power during periods of low generation or peak demand. This balancing action stabilizes the power supply and reduces the operating hours and fuel consumption of diesel generators, resulting in lower emissions and operational costs [16], [17]. Battery systems are typically managed using bidirectional DC-DC converters to control charging and discharging processes effectively [18]. Maximizing energy extraction from renewable sources is critical for the efficiency and reliability of hybrid microgrids. Solar PV systems commonly employ boost converters combined with Maximum Power Point Tracking (MPPT) algorithms such as the Perturb and Observe method to maximize power output under varying irradiance and temperature conditions [19], [20]. Wind energy conversion systems typically use Permanent Magnet Synchronous Generators with MPPT control to optimize energy capture at different wind speeds [21], [22]. These MPPT methods enhance the overall energy yield and operational efficiency of renewable subsystems. Maintaining high power quality and frequency stability remains a challenge in hybrid microgrids due to the variable nature of renewable energy generation and fluctuating loads [23]. Traditional control methods may not adequately handle the complex dynamics of such systems or ensure smooth power sharing among multiple sources. Advanced control techniques, including cascaded Generalized Second-Order Integrator based Phase-Locked Loops

(C-SOGI PLL), have been shown to provide accurate grid synchronization, harmonic filtering, and robust frequency tracking [24], [25]. These advanced controls improve the dynamic response of the microgrid, reduce total harmonic distortion, and ensure the safe operation of sensitive electrical loads. This paper proposes a comprehensive hybrid AC microgrid architecture that integrates solar PV, wind turbines, battery storage, and diesel generators, combined with advanced control strategies including MPPT and C-SOGI PLL. The goal is to significantly reduce diesel generator fuel consumption and emissions while ensuring reliable, stable, and high-quality power supply to connected loads. The system's effectiveness is validated through MATLAB/Simulink simulations which demonstrate improvements in load balancing, frequency regulation, power quality, and operational cost savings when compared to conventional control methods.

2. System Configuration

The proposed hybrid AC microgrid system combines solar photovoltaic (PV) panels, a wind energy conversion system, a diesel generator, and a battery energy storage system to provide a reliable, stable, and efficient power supply. The solar PV subsystem is connected to the DC bus via a DC-DC boost converter, while the wind energy subsystem converts wind energy into electrical power. The battery energy storage system dynamically charges or discharges based on real-time energy availability and load demand, maintaining system balance and providing backup during renewable shortages. The diesel generator interfaces with the AC bus and serves as a backup energy source during low renewable generation or battery depletion. To improve power quality and minimize harmonic injection, an LC filter is employed on the diesel generator output side. A cascaded Generalized Second-Order Integrator-based Phase-Locked Loop (C-SOGI PLL) is implemented for accurate synchronization and control. The control architecture coordinates all energy sources through an intelligent power management strategy, prioritizing renewable utilization, supporting peak loads with batteries, and activating the diesel generator only when necessary. The system is extensively modeled and simulated using MATLAB/Simulink to validate its performance in harmonic suppression, load balancing, dynamic response, frequency regulation, and cost-effectiveness.

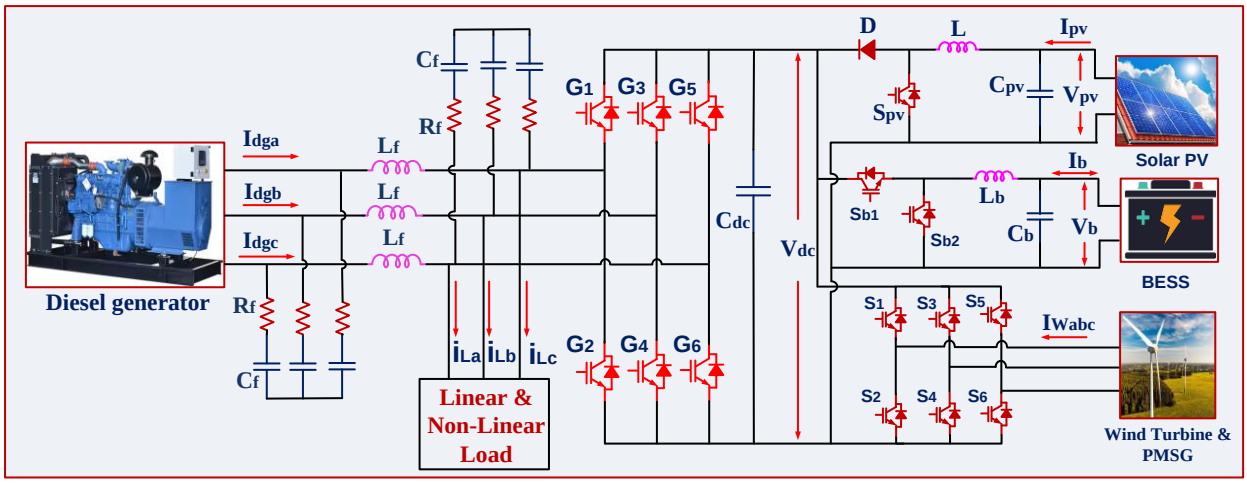

Fig. 1 Proposed AC-Microgrid configuration.

3. Modeling and Designing of proposed Hybrid AC Microgrid

A. Designing of Diesel Generator Configuration

In the proposed hybrid AC microgrid system, the diesel generator plays a crucial role in ensuring system reliability and continuous power supply, especially during periods of insufficient renewable generation. The generator operates in standby mode under normal conditions when the combined power output from solar photovoltaic, wind energy, and battery storage adequately meets the load demand. However, when renewable sources are unable to supply power due to climatic variations such as reduced solar irradiance or low wind speeds, and when the battery's state of charge falls below a predefined threshold, the diesel generator is automatically activated to maintain system stability

and meet the required load. Once activated, the diesel engine converts chemical energy from fuel combustion into mechanical energy, which is then used to drive a synchronous generator that produces three-phase alternating current as shown in Fig.2. To ensure high power quality, this AC output is passed through an LC filter, which effectively attenuates high-frequency harmonics. In this system configuration, the AC power generated by the diesel generator is further converted into direct current through an AC to DC converter to interface with the common DC bus, enabling integrated operation with other DC-linked renewable sources and battery storage. This approach not only enhances the dynamic power balancing capability of the microgrid but also reduces the excessive use of diesel fuel, thereby lowering operating costs and minimizing environmental impact.

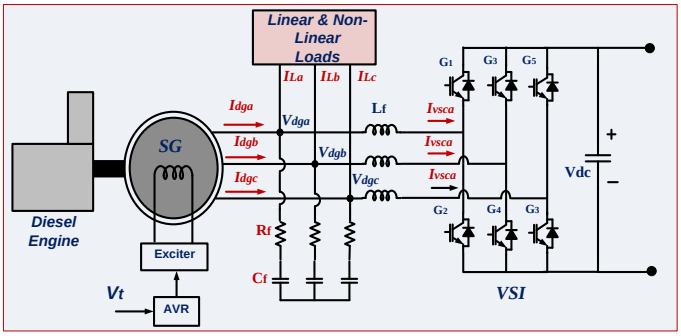

Fig. 2. AVR controller with DC excitation.

The diesel generator consists of two primary components:

1. Diesel Engine (Prime Mover)
2. Synchronous Generator (Electrical Generator)

This system converts chemical energy (from fuel) to mechanical energy (via combustion) and finally to electrical energy using a rotating electrical machine.

1. Diesel Engine Modeling (Mechanical Dynamics)

The diesel engine produces torque which drives the generator. The mechanical dynamic equation governing this behavior is:

$$J\frac{d\omega_m}{dt} = T_m - T_e - D\omega_m \quad (1)$$

Where:

- J: Rotor inertia (kg·m²)
- ωm: Rotor angular speed (rad/s)
- Tm: Mechanical torque produced by the engine (Nm)
- Te: Electromagnetic torque by the generator (Nm)
- D: Damping coefficient

The mechanical power is:

$$P_m = T_m \cdot \omega_m \quad (2)$$

2. Synchronous Generator Modeling

A three-phase synchronous generator is used to convert mechanical energy to AC electrical energy. d–q Axis Voltage Equations (Park's Transformation)

$$v_d = R_s i_d + \frac{d\lambda_d}{dt} - \omega\lambda_q \quad (3)$$

$$v_q = R_s i_q + \frac{d\lambda_q}{dt} - \omega\lambda_d \quad (4)$$

Where:

- vd,vq: d-q axis voltages
- id,iq: d-q axis currents
- λd,λq: d-q axis flux linkages
- Rs: Stator resistance
- ω: Electrical angular speed

3. Flux Linkages

$$\lambda_d = L_d i_d + \lambda_f \quad (5)$$

$$\lambda_q = L_q i_q \quad (6)$$

Where:

- Ld,Lq: d-q axis inductances
- λf: Field flux linkage

Electromagnetic Torque

$$T_e = \frac{3}{2}\cdot\frac{P}{2}\cdot\left(\lambda_d i_q - \lambda_q i_d\right) \quad (7)$$

Where P is the number of poles.

4. AC to DC Conversion (Interface with DC Bus)

To supply the DC bus, the AC output is rectified using:

$$V_{DC} = \frac{3\sqrt{2}}{\pi} V_{LL} \cdot \cos(\alpha) \quad (8)$$

Where α is the firing angle for IGBTs.

5. Harmonic Reduction with LC Filter

An LC filter is used on the AC side (between generator and rectifier) to reduce harmonics before rectification.

Cut-off Frequency:

$$f_r = \frac{1}{2\pi\sqrt{LC}} \quad (9)$$

a. Inductor Value (L)

To limit the ripple current or reduce harmonics, the inductor can be estimated as:

$$L = \frac{V_{ph}}{4\pi f I_{ripple}} \quad (10)$$

Where:

- Vph = Phase voltage (V)
- f = System frequency (Hz)
- Iripple = Allowed ripple current (usually 10–30% of load current)

b. Capacitor Value (C)

To filter high-frequency content and maintain voltage stability:

$$C = \frac{1}{(2\pi f_c)^2 L} \quad (11)$$

B. Solar PV boost converter system configuration

The solar power system in a AC microgrid is crucial for efficient energy conversion and integration with other renewable energy sources. A perturb and observe (P&O) maximum power point tracking (MPPT) boost converter is used to optimize power extraction from the photovoltaic (PV) array, ensuring it operates at its maximum power point under varying solar irradiance conditions as shown in Fig.3. The P&O MPPT algorithm continuously adjusts the operating point by introducing small perturbations to the duty cycle of the DC-DC boost converter. This architecture ensures stable power distribution for EV fast charging stations, minimizing power losses and improving overall efficiency. The DC microgrid benefits from this configuration by achieving improved renewable energy utilization, reduced reliance on grid power, and enhanced power quality. The bidirectional energy flow capability allows for effective integration with battery storage systems, ensuring energy availability even during low solar generation periods. Implementing this solar P&O MPPT boost converter allows the DC microgrid to manage power distribution, support multiple EV chargers, and enhance sustainability by reducing carbon emissions through increased renewable energy penetration.

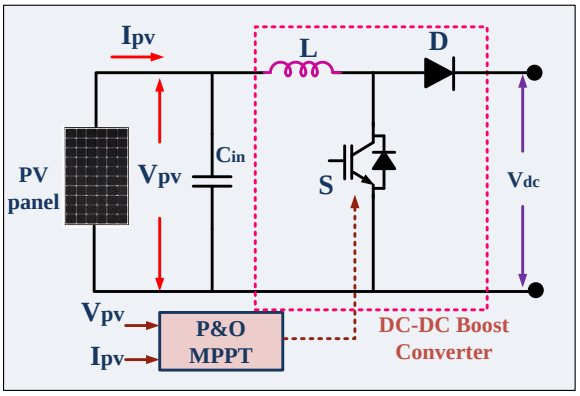

Fig. 3 solar PV P&O MPPT DC-DC boost converter

1. Single-Diode Solar PV Model: Designing a single-diode solar PV model involves analyzing the electrical characteristics of a photovoltaic (PV) cell. The single-diode model is one of the most commonly used to simulate the behavior of a PV cell. This model includes one diode, a current source, and series and shunt resistances to represent losses as shown in fig.4.
2. Basic Equation of the Single-Diode Model: The equation that governs the behavior of the single-diode PV model is derived from Kirchhoff's current law (KCL):

$$I = I_{Ph} - I_D - I_{sh} \quad (12)$$

Where: I = output current of the PV module (A), Iph = photocurrent, the current generated by light (A), ID = diode current (A), Ish = shunt current (A)

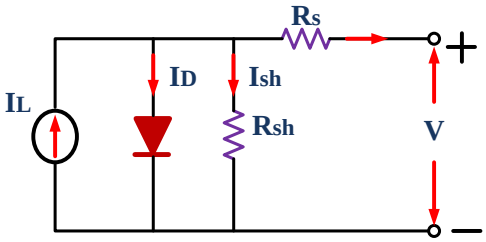

Fig. 4 equivalent model of PV solar.

3. Diode Current (ID): The current through the diode is described by the Shockley diode equation:

$$I_D = I_0\left(e^{\frac{V+IR_s}{nV_t}} - 1\right) \quad (13)$$

Where: I_0 = reverse saturation current of the diode (A), V = voltage across the PV cell (V), R_s = series resistance (Ω), n = diode ideality factor (typically between 1 and 2), V_t = thermal voltage (V), given by V_t=qkT

Here: k = Boltzmann constant (1.38×10^{-23} J/K), T = temperature in Kelvin (K), q = electron charge (1.6×10^{-19} C)

4. Shunt Current (Ish): The current through the shunt resistance Rsh is modeled as:

$$I_{sh} = \frac{V+IR_S}{R_{sh}} \quad (14)$$

5. Equation of the Single-Diode PV Model: By substituting the expressions for ID and Ish into the main current equation, we get the complete form of the single-diode model:

$$I = I_{Ph} - I_0\left(e^{\frac{V+IR_S}{nV_t}} - 1\right) - \frac{V+IR_S}{R_{sh}} \quad (15)$$

6. Photo current I_{Ph}: The current generated by the cell due to light is proportional to the incident light and is affected by temperature. It can be modeled as:

$$I_{ph} = \left[I_{ph,ref} + \mu I_{Ph} \cdot \left(T - T_{ref}\right)\right] \cdot \frac{G}{G_{ref}} \quad (16)$$

Where: $I_{ph,ref}$ = reference photocurrent at standard test conditions (STC), I_{Ph} = temperature coefficient of photocurrent (A/°C), T = cell temperature (°C), T_{ref} = reference temperature (usually 25°C), G = irradiance (W/m²), G_{ref} = reference irradiance at STC (1000 W/m²)

7. Saturation Current I_0: The reverse saturation current varies exponentially with temperature:

$$I_0 = I_{0,ref}\left(\frac{T}{T_{ref}}\right)^3 e^{\frac{Eg}{nV_t}\left(\frac{1}{T_{ref}} - \frac{1}{T}\right)} \quad (17)$$

Where:, $I_{0,ref}$ = reverse saturation current at reference temperature, Eg = bandgap energy of the semiconductor (typically 1.1 eV for silicon)

C. P&O MPPT algorithm designing

The **Perturb and Observe (P&O) Maximum Power Point Tracking (MPPT) Algorithm** is one of the most widely used techniques for extracting maximum power from a solar photovoltaic (PV) system. It works by periodically perturbing the PV voltage and observing the resulting change in power to track the Maximum Power Point (MPP) as shown in Fig.5. The algorithm operates by making small perturbations (increment or decrement) to the PV voltage (Vpv) and observing the corresponding change in power (Ppv). Based on the response, it adjusts the duty cycle of the DC-DC boost converter to move towards the MPP.

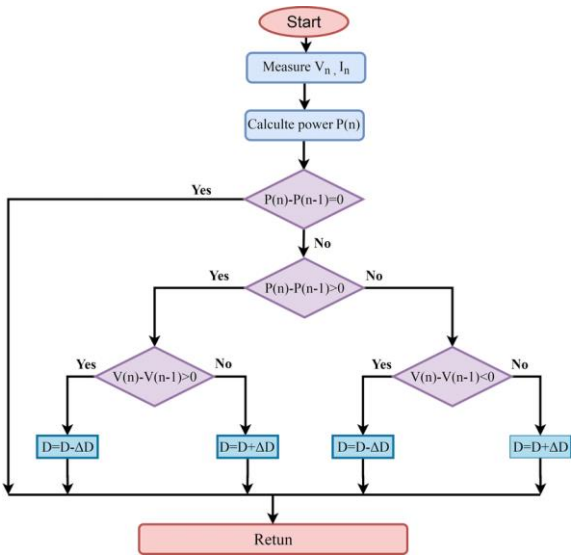

Fig.5 flow chart of P&O MPPT algorithm

1. Calculate Power Output:

$$P_{Pv} = V_{Pv} \times I_{Pv} \quad (18)$$

Where: Vpv = PV panel output voltage, Ipv = PV panel output current, Ppv = PV panel output power

2. Compare Current and Previous Power:

$$\text{ch arg}e\ in\ Poωer : \Delta P = P_{Pv}(t) - P_{Pv}(t-1) \quad (19)$$

$$\text{ch arg}e\ in\ Voltage : \Delta V = V_{Pv}(t) - V_{Pv}(t-1) \quad (20)$$

3. Decision Conditions:

$$if \Delta P > 0 and \Delta V > 0 \rightarrow increaseVoltage \quad (21)$$

$$if \Delta P > 0 and \Delta V < 0 \rightarrow decrease\ Voltage \quad (22)$$

$$if \Delta P < 0 and \Delta V > 0 \rightarrow decrease\ Voltage \quad (23)$$

$$if \Delta P < 0 and \Delta V < 0 \rightarrow increaseVoltage \quad (24)$$

4. Duty Cycle (D) of Boost Converter:

- The new duty cycle is adjusted based on the voltage perturbation decision.
- The boost converter duty cycle is given by:

$$D = 1 - \frac{V_{pv}}{V_{dc}} \quad (25)$$

Where: Vdc= Output voltage of the boost converter

D. Designing of battery conversion configuration in AC Microgrid

In an AC microgrid system, the DC-DC bidirectional buck-boost converter plays a vital role in facilitating controlled energy exchange between the battery energy storage system (BESS) and the DC bus that interconnects

renewable sources (like solar PV and wind), diesel generators, and the grid interface. This converter allows bidirectional power flow, operating in either buck mode or boost mode, depending on the energy requirements of the microgrid. When there is excess renewable energy generation (i.e., solar or wind output exceeds the load demand), the converter operates in buck mode, reducing the higher DC bus voltage to a suitable lower level for charging the battery. Conversely, during periods of low renewable generation or high load demand, the converter shifts to boost mode, drawing power from the battery and raising its lower voltage to match the DC bus level, thus discharging the battery to support the load or maintain bus voltage stability. The converter uses a combination of power MOSFETs or IGBTs, along with inductors and capacitors, and is controlled by pulse width modulation (PWM) schemes to precisely regulate voltage and current flow. A control algorithm monitors the State of Charge (SOC) of the battery and the DC bus voltage, making real-time decisions to either charge or discharge the battery as needed. This ensures efficient load balancing, voltage regulation, and system resilience under dynamic operating conditions. Moreover, in coordination with renewable sources and diesel generators, the bidirectional converter helps in optimizing fuel usage, improving power quality, and ensuring uninterrupted supply to critical loads within the microgrid.

1. Buck Mode (Battery Charging)

Output Voltage in Buck Mode:

$$V_b = D \cdot V_{dc} \quad (26)$$

Where: Vb = Battery voltage, Vdc = DC bus voltage, D = Duty cycle (0<D<1)

Inductor Current Ripple in Buck Mode:

$$\Delta I_L = \frac{(1-D)V_{dc}}{Lf_s} \quad (27)$$

Where: ΔIL = Inductor current ripple, L = Inductor value, fs = Switching frequency

2. Boost Mode (Battery Discharging)

Output Voltage in Boost Mode:

$$V_{dc} = \frac{V_b}{1-D} \quad (28)$$

Inductor Current Ripple in Boost Mode:

$$\Delta I_L = \frac{DV_b}{Lf_s} \quad (29)$$

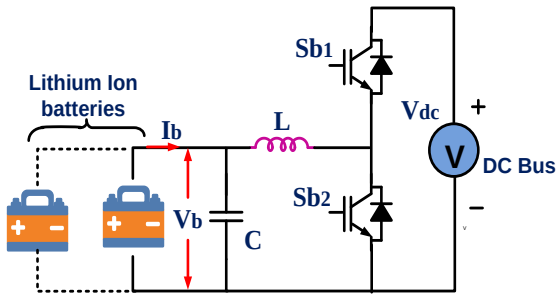

Fig.6 principle operation bidirectional dc-dc buck boost converter

E. Double-Loop PI Control Strategy for battery storage system

The AC microgrid, which integrates various energy sources like solar PV, wind turbines, diesel generators, and battery storage, requires effective voltage regulation and energy flow control for system stability and performance. A double-loop control strategy is used for the DC-DC bidirectional buck-boost converter, connecting the battery energy storage system to the DC bus. This control scheme consists of two cascaded loops: an outer voltage control loop and an inner current control loop. The outer loop regulates the DC bus voltage by comparing the measured DC voltage with a predefined reference value, while the inner current loop compares this with the actual battery current. A second PI controller minimizes current error by adjusting the duty cycle of the converter switch, effectively managing power flow into or out of the battery as shown in Fig.7. This dual-loop configuration allows fast dynamic response and precise control over voltage and current, enhancing power quality and extending battery life by enforcing smooth and controlled charging and discharging operations.

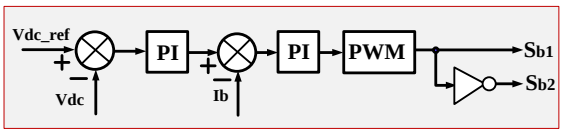

Fig. 7 double loop battery charging controller

1. Outer Loop – DC Bus Voltage Control

- The outer loop maintains constant DC bus voltage (Vdc_ref).
- Output: Generates the reference current Ibref for the inner loop.

Voltage Error:

$$e_v(t) = V_{dc}^{ref} - V_{dC}(t) \quad (30)$$

PI Controller Output (Reference Battery Current):

$$I_b^{ref}(t) = K_{pv}e_v(t) + k_{iv}\int e_v(t)dt \quad (31)$$

Where:

- Kpv: Proportional gain for voltage controller
- Kiv: Integral gain for voltage controller

2. Inner Loop – Battery Current Control

- The inner loop controls battery current Ib based on Ibref.

Current Error:

$$e_i(t) = I_b^{ref} - I_b(t) \quad (32)$$

PI Controller Output (Duty Cycle D):

$$D(t) = K_{p_i}e_i(t) + K_{ii}\int e_i(t)dt \quad (33)$$

Where:

- Kpi: Proportional gain for current controller
- Kii: Integral gain for current controller

This duty cycle D is then applied to the PWM gate signal of the bidirectional converter's switches.

F. Designing of Wind Conversion System

The wind energy conversion system operates by harnessing the kinetic energy of the wind through a wind turbine and converting it into electrical energy using a Permanent Magnet Synchronous Generator, or PMSG. When wind flows over the turbine blades, aerodynamic lift is produced, causing the rotor to rotate. This rotational mechanical energy is transmitted to the shaft of the PMSG, which generates three-phase alternating current electrical power. However, the voltage and frequency of this AC power vary with wind speed, making it unsuitable for direct use in the microgrid. To manage this, the generated AC power is first converted into direct current through a rectifier. To ensure that the maximum possible power is extracted from the wind at all speeds, a Maximum Power Point Tracking technique, often the Perturb and Observe or Tip Speed Ratio method is applied. This technique continuously adjusts the operating point of the converter to track and capture the highest available power from the wind as shown in Fig.8. The resulting DC power is then regulated and used to supply the DC bus or to charge battery storage systems. This regulated power supports the microgrid load demand and helps reduce reliance on traditional sources like diesel generators, thereby improving system efficiency and promoting the use of renewable energy.

In this configuration, a wind turbine is mechanically coupled to a Permanent Magnet Synchronous Generator (PMSG). The electrical output of the PMSG is a variable-frequency AC that is first rectified to DC and then converted back to AC through a Voltage Source Inverter (VSI) for AC load/grid interface or directly supplied to the DC bus of the microgrid.

1. Wind Turbine Power Output:

The mechanical power extracted from wind is given by:

$$P_{wind} = \frac{1}{2} \cdot \rho \cdot A \cdot v^3 \cdot C_P(\lambda, B) \quad (34)$$

Where: ρ = Air density (kg / m^3), $A = \pi R^2$ swept area of turbine blades, v = wind speed (m/s), C_P = power coefficient (function of tip speed ratio λ and pitch angle β)

2. Tip Speed Ratio λ:

$$\lambda = \frac{\omega_t R}{v} \quad (35)$$

Where: ω_t: Turbine angular speed (rad/s), R: Blade radius (m)

3. PMSG Modeling (dq-axis):

PMSG electrical dynamics in dq-frame:

$$V_d = R_s i_d + \frac{d\psi_d}{dt} - \omega_e \psi_q \quad (36)$$

$$V_q = R_s i_q + \frac{d\psi_q}{dt} - \omega_e \psi_d \quad (37)$$

$$T_e = \frac{3}{2} P\left(\psi_d i_q - \psi_q i_d\right) \quad (38)$$

Where: R_s: Stator resistance, ψ_d,ψ_q: d and q-axis flux linkages, ω_e : Electrical angular speed, T_e : Electromagnetic torque, P: Number of pole pairs

4. Control on the Machine Side

The machine-side control relies heavily on wind speed reference generation in order to get the most power out of the wind turbine. Figure 5 shows the control circuit of an active rectifier-connected PMSG. The ideal ratio of tip speed to actual wind speed is used to determine the reference rotor speed. This is the reference speed:

$$\omega_m^{opt} = \frac{\lambda'_{opt} v_w}{R} \quad (39)$$

The speed of the reference rotor is represented by ω_m^{opt}. The PI speed controller is used to limit the speed error, which is calculated from the ideal wind speed and the actual speed of the PMSM, as reference electromagnetic torque. This means:

$$\omega_r^{error} = \omega_m^{opt} - \omega_r \quad (40)$$

$$T_e^* = k_{p,s}(\omega_r^{error}) + k_{i,s}\int (\omega_r^{error})\, dt \quad (41)$$

The variables ω_r^{error}, T_e^*, $k_{p,s}$, and $k_{i,s}$ denote the rotor speed error, reference electromagnetic torque, proportional gain, and integral gain, respectively, of the speed controller.

The reference q-axis current (i_{qm}^*) is:

$$i_{qm}^* = \frac{4T_e^*}{3P} \quad (42)$$

An inner loop current controller regulates the machine side converter, which in turn generates the reference voltage. The coordinates on the d-q axis are:

$$v_{dm}^* = k_{p,mc}(i_{dm}^* - i_{ds}) + k_{i,mc}\int (i_{dm}^* - i_{ds})\, dt - \omega_e L_s i_{qs} \quad (43)$$

$$v_{qm}^* = k_{p,mc}(i_{qm}^* - i_{qs}) + k_{i,mc}\int (i_{qm}^* - i_{qs})\, dt + \omega_e(L_s i_{ds} + \lambda_m) \quad (44)$$

The variables v_{dm}^* and v_{qm}^* on the d-q axis represent the reference machine voltage, i_{dm}^* and i_{qm}^* on the d-q axis represent the reference stator current, and the variables $k_{p,mc}$ and $k_{i,mc}$ represent the component gains of the machine current controller, respectively.

The voltage references on the d-q axis are converted into three-phase machine voltage references via inverse park transformation so that the wind turbine can produce its maximum output. Pulse width modulation (PWM) generators use these three-phase machine voltage references and use them to operate the active rectifier on the machine side.

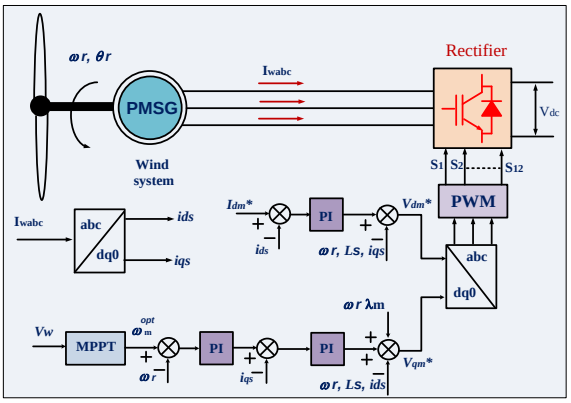

Fig.8 Wind conversion controller

4. Designing of Diesel Generator AC-DC controller

A diesel generator integrated into the AC microgrid is regulated through a voltage source inverter (VSI), which converts the generator's AC output to a controlled DC voltage, allowing seamless connection to the DC bus and power sharing with renewable sources. To ensure efficient operation and stable power delivery, a hysteresis voltage control technique is used for the inverter. This control method maintains the output voltage of the diesel generator within a predefined hysteresis band, enabling rapid dynamic response and accurate voltage regulation under varying load conditions as shown in Fig.9. The controller adjusts the switching of the inverter based on real-time voltage deviation, ensuring that the generator supplies only the required power to maintain system stability, particularly when renewable sources are insufficient. An LC filter is implemented at the inverter output to smooth the voltage waveform and eliminate high-frequency harmonics generated by switching operations. This setup enhances power quality, maintains voltage consistency across the microgrid, and supports effective load balancing. By regulating the diesel generator's contribution only when necessary, the controller minimizes fuel consumption and extends the operational life of the generator while ensuring reliable backup power.

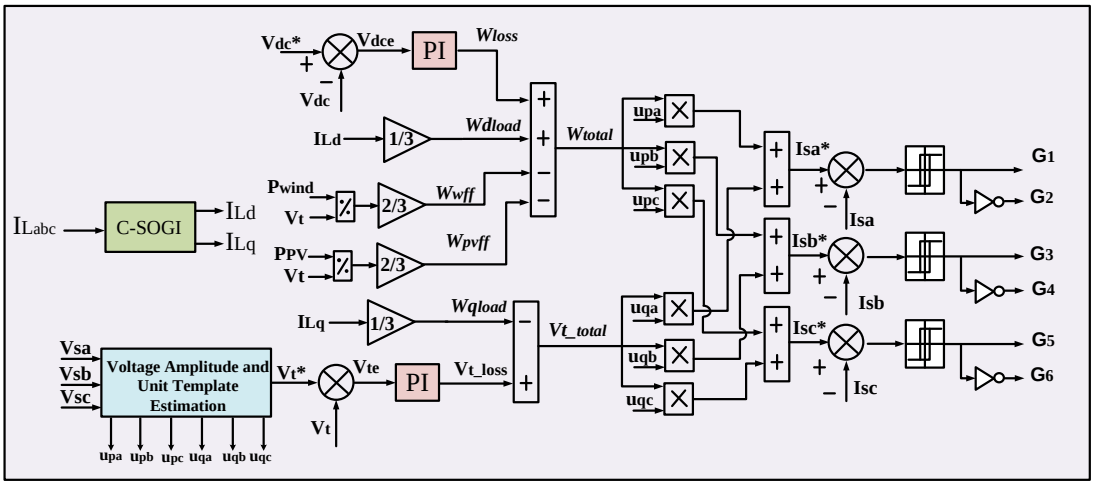

Fig. 9 Control strategy of diesel generator voltage source converter

1. *DC Loss Component Estimation*

A Proportional–Integral (PI) controller is utilized to regulate the DC link voltage at the output of the diesel generator-side voltage source converter (VSC) in a hybrid AC microgrid. The VSC is responsible for converting the diesel generator's AC output into DC power, which is then supplied to the common DC bus. Due to variations in load demand and interactions with renewable energy sources, maintaining a stable DC voltage is critical for system reliability and coordinated power sharing. The PI controller continuously monitors the error between the reference DC voltage and the actual DC bus voltage. The proportional term ensures a fast transient response, while the integral term eliminates steady-state error by integrating the error over time. The combined PI output modulates the gating signals of the VSC switches to regulate the power flow and stabilize the DC link voltage. This control strategy supports dynamic voltage regulation, reduces ripple, and ensures compatibility with other DC-connected sources and loads in the microgrid, thereby improving system performance and operational efficiency.

$$V_{dce} = V_{dc}^{*} - V_{dc} \qquad (45)$$

2) Estimation of Feed-Forward Components of RERs

The DC link voltage control system's dynamic response is enhanced by using feed-forward terms linked to renewable energy resources (RERs), such as solar and wind. These terms are calculated based on real-time power output, allowing the controller to anticipate changes in power flow to the DC link. These terms are derived from monitoring variations in solar irradiance and wind speed, which directly impact the power generated by solar panels and wind turbines. By incorporating these terms into the control strategy, the system can preemptively adjust the voltage source converter (VSC) operation, ensuring stable DC link voltage despite fluctuations in renewable energy generation. This reduces reliance on feedback control and improves dynamic performance.

$$w_{PVff} = \frac{2P_{PV}}{3V_t} \qquad (46)$$

$$w_{wff} = \frac{2P_{wind}}{3V_t} \qquad (47)$$

Where, P_{PV}, w_{PVff}, P_{wind}, w_{wff} are the PV power and feed-forward term, wind power and its feed-forward term, respectively.

3) Structure of C-SOGI Prefilter Based SRF- PLL

In a diesel generator-integrated AC microgrid, the load current sensing and transformation are crucial for synchronization and control. The generator's terminal voltages and load currents are initially in the three-phase (abc) reference frame, and these need to be converted into the rotating dq0 reference frame for effective voltage and current regulation. This process involves two primary transformations: Clarke Transformation (abc-$\alpha\beta$) and Park Transformation ($\alpha\beta$-dq0). Accurate detection of the voltage angle (θ) is essential, and for this purpose, a Synchronous Reference Frame Phase Locked Loop (SRF-PLL) with a Complex Second-Order Generalized Integrator (C-SOGI) prefilter is used. The C-SOGI acts as a voltage signal conditioner,

filtering out DC offset and high-frequency harmonics from the measured voltage before it is fed into the PLL loop. This enhances the robustness and accuracy of θ and frequency (f) detection, particularly under unbalanced or distorted grid conditions.

abc to αβ Transformation (Clarke Transformation)

$$\begin{bmatrix} i_\alpha \\ i_\beta \end{bmatrix} = \frac{2}{3}\begin{bmatrix} 1 & -\frac{1}{2} & -\frac{1}{2} \\ 0 & \frac{\sqrt{3}}{2} & -\frac{\sqrt{3}}{2} \end{bmatrix}\begin{bmatrix} i_a \\ i_b \\ i_c \end{bmatrix} \quad (48)$$

This gives the stationary orthogonal components iα,iβ from the three-phase current values ia,ib,ic.

αβ to dq Transformation (Park Transformation)

Using the angle θ obtained from the PLL:

$$\begin{bmatrix} i_d \\ i_q \end{bmatrix} = \begin{bmatrix} \cos(\theta) & \sin(\theta) \\ -\sin(\theta) & \cos(\theta) \end{bmatrix}\begin{bmatrix} i_\alpha \\ i_\beta \end{bmatrix} \quad (49)$$

Where:

- id represents the direct-axis current (active power component)
- iq represents the quadrature-axis current (reactive power component)

Structure and Transfer Function of C-SOGI-based SRF-PLL

The C-SOGI filters the diesel generator voltage vs into in-phase vα and quadrature vβ components with improved noise and harmonic rejection.

C-SOGI Transfer Functions:

$$G_{c-SOGI}(s) = \frac{k\omega s}{S^2+k\omega s+\omega^2} \quad (50)$$

Where:

- k is the C-SOGI gain (typically k=1.414 for critical damping),
- ω is the nominal grid angular frequency ω=2πf

The angle tracking loop of SRF-PLL uses a PI controller with:

$$G_{ol}(s) = \left(k_p + \frac{k_i}{s}\right)\cdot\frac{1}{s} \quad (51)$$

$$G_{cl}(s) = \frac{k_p s+k_i}{s^2+k_p s+k_i} \quad (52)$$

Where:

- kp and ki are the proportional and integral gains of the PI controller,
- These can be tuned using symmetrical optimum or pole-zero cancellation methods for desired bandwidth and damping.

4) Unit template voltage estimation

The net active reference current, can now be represented as

$$w_{total} = w_{loss} + w_{dload} - w_{wff} - w_{pvff} \quad (53)$$

The phase voltages (V_{abc}) are computed from the line voltages as

$$\begin{bmatrix} v_{sa} \\ v_{sb} \\ v_{sc} \end{bmatrix} = \frac{1}{3}\begin{bmatrix} 2 & 1 & 0 \\ -1 & 1 & 0 \\ -1 & -2 & 0 \end{bmatrix}\begin{bmatrix} v_{Lab} \\ v_{Lbc} \\ 0 \end{bmatrix} \quad (54)$$

$$V_t = \sqrt{\frac{2(V_{sa}^2+V_{Sb}^2+V_{sc}^2)}{3}} \quad (55)$$

$$u_{pa} = v_{sa} / V_t \quad ; \quad u_{pb} = v_{sb} / V_t \quad ; \quad u_{pc} = v_{sc} / V_t \quad (56)$$

$$u_{qa} = -\frac{u_{pb}}{\sqrt{3}} + \frac{u_{pc}}{\sqrt{3}}; u_{qb} = \frac{\sqrt{3}u_{pa}}{2} + \frac{(u_{pb}-u_{pc})}{2\sqrt{3}}; u_{qc} = -\frac{\sqrt{3}u_{pa}}{2} + \frac{(u_{pb}-u_{pc})}{2\sqrt{3}} \quad (57)$$

Line terminal voltage error represented as

$$V_{tc} = V_t^* - V_t \quad (58)$$

5) Generation of Gate Pulses for VSC: Finally, the reference currents for source DG, for supplying power to the load at night, are obtained by multiplying its unit templates

$$i_{sa}^* = w_{total} \times u_{pa} + w_{total} \times u_{qa} \quad (59)$$

$$i_{sb}^* = w_{total} \times u_{pb} + w_{total} \times u_{qb} \quad (60)$$

$$i_{sc}^* = w_{total} \times u_{pc} + w_{total} \times u_{qc} \quad (61)$$

By feeding the error between reference currents and sensed grid voltage source converter currents, a three phase hysteresis relay produces gate pulses for the switches in upper leg of grid side VSC. The complementary signal is used for switching the lower leg of the grid side VSC.

5. Simulation Results and Discussion

To evaluate the dynamic performance and energy-sharing capability of the proposed hybrid AC microgrid, a simulation was conducted in MATLAB/Simulink for a total duration of 0.8 seconds. The system includes a diesel generator with a capacity of 100 kW, a solar PV unit with a capacity of 20 kW, a wind turbine generator rated at 20 kW, and a battery energy

storage system with a capacity of 180 kW. The total load demand is 62 kW, comprising both linear and nonlinear loads. The entire system is synchronized using a C-SOGI-based SRF-PLL to maintain power quality and system stability. In the first 0.2 seconds, the solar irradiance is 1000 W/m², and the wind speed is 12 m/s. Under these conditions, the solar PV and wind generator both produce their maximum output of 20 kW each. With a total renewable contribution of 40 kW, the diesel generator supplies 12 kW to meet the total load demand of 62 kW, and the battery remains idle as no compensation is required. This period represents optimal renewable generation with minimal diesel utilization. From 0.2 to 0.3 seconds, the solar irradiance decreases from 1000 to 500 W/m², reducing the solar power output from 20 kW to 10 kW. To maintain power balance, the battery discharges 10 kW while the wind generator continues to generate 20 kW. Between 0.3 and 0.6 seconds, the solar irradiance further declines from 500 W/m² to zero, resulting in zero solar generation. During this interval, the battery compensates by discharging an additional 10 kW, reaching a total of 20 kW battery discharge to support the load. Simultaneously, the wind speed drops from 12 m/s to 10 m/s between 0.3 and 0.4 seconds, causing the wind power output to decrease from 20 kW to 10 kW. The wind speed then falls further to 0 m/s from 0.4 to 0.5 seconds, halting wind power generation completely. In response, the battery discharges another 10 kW to make up for the deficit, resulting in a total of 40 kW battery discharge during this critical interval when both solar and wind sources are unavailable. From 0.5 to 0.6 seconds, the wind speed increases from 0 m/s to 10 m/s, allowing the wind generator to gradually recover and produce 10 kW of power. From 0.6 to 0.8 seconds, the wind speed rises from 10 m/s to 12 m/s, restoring the wind generation back to its full capacity of 20 kW. During the same time, solar irradiance also recovers. From 0.6 to 0.7 seconds, it increases from 0 to 500 W/m², and from 0.7 to 0.8 seconds, it rises from 500 to 1000 W/m². Consequently, solar generation ramps up from 0 to 10 kW and then to its full capacity of 20 kW. As the solar and wind sources regain their generation capabilities, the battery transitions from discharging to charging mode. The diesel generator maintains a consistent 12 kW output throughout the simulation, ensuring uninterrupted load supply even during renewable generation drops. The dynamic coordination among renewable sources, battery storage, and diesel generator ensures a continuous and stable power supply to the load. Figure 10 illustrates the time-domain performance of all the power sources, confirming that the proposed hybrid energy system operates effectively under varying climatic conditions. The results demonstrate that the system maintains power balance, supports the load during renewable power fluctuations, and uses the diesel generator as a backup with minimal fuel consumption. This validates the reliability, flexibility, and efficiency of the proposed hybrid energy management strategy.

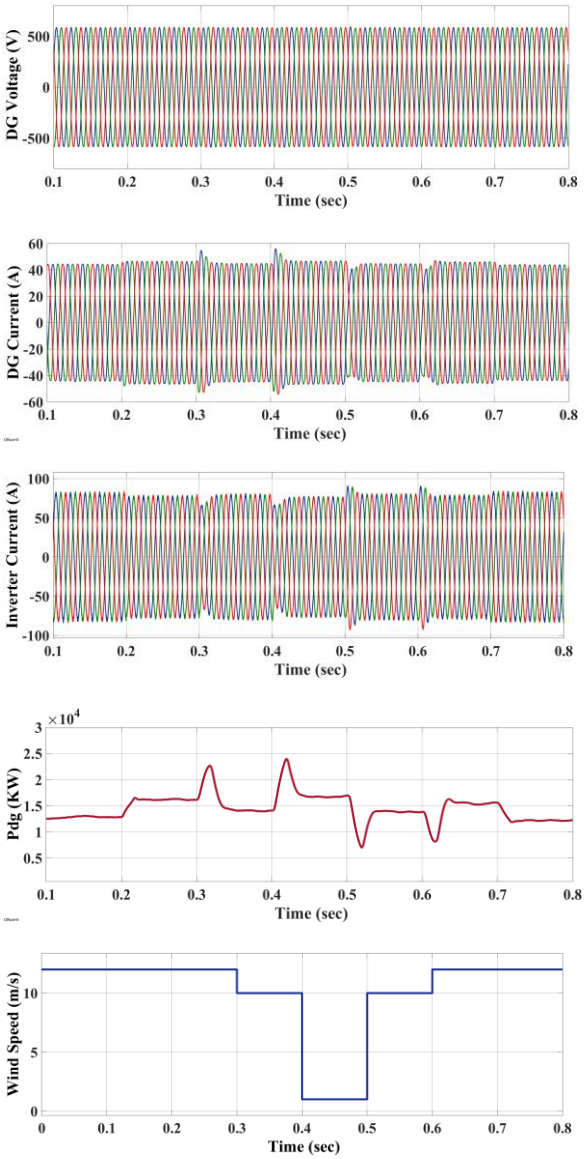

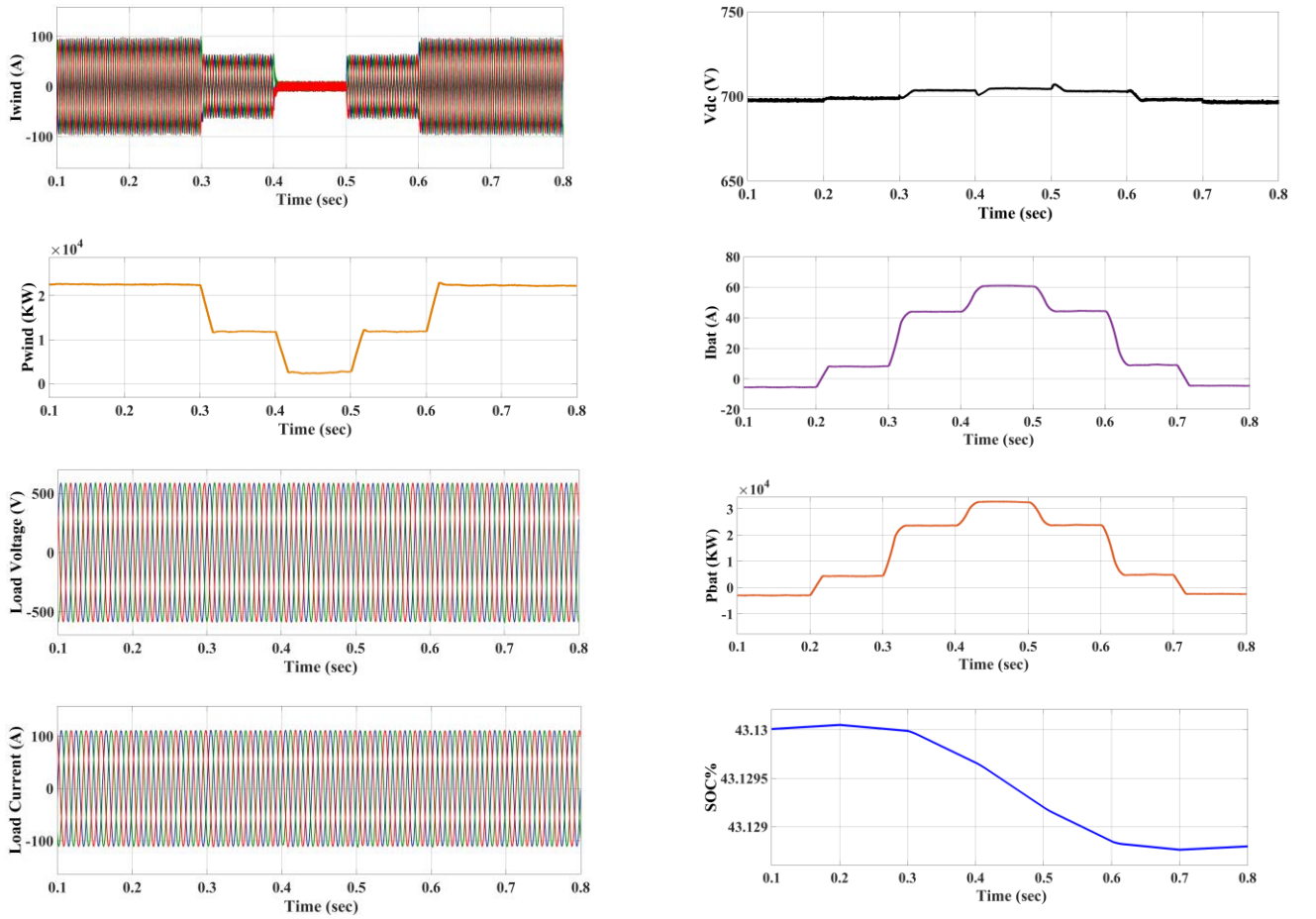

Fig.10 Simulation results of the Proposed Hybrid AC Microgrid under Dynamic Solar and Wind Variations with Coordinated Diesel Generator and Battery Support

The Total Harmonic Distortion (THD) of the diesel generator is well within acceptable limits, with a voltage THD of 1.42% and a current THD of 0.65%, demonstrating the effectiveness of the proposed control strategy in maintaining power quality across the microgrid as shown in Fig.11.

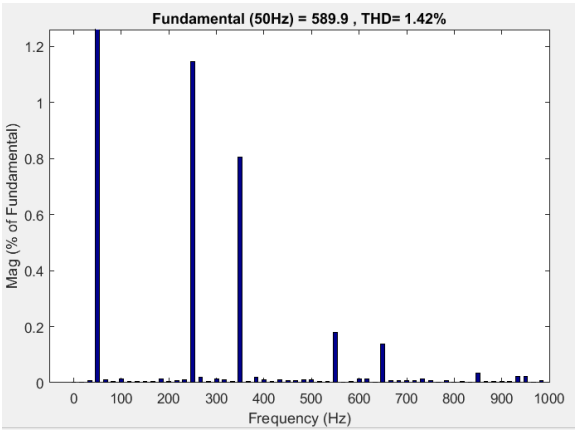

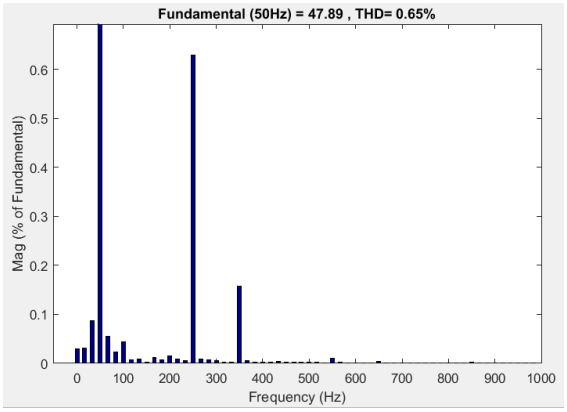

Fig. 11. FFT results for DG Genset parameters.

6. Conclusion

The paper presents a hybrid AC microgrid architecture that combines solar PV, wind turbines, a battery energy storage system (BESS), and a diesel generator to improve power quality, frequency regulation, and operational efficiency. The system prioritizes renewable energy utilization through MPPT-based control, a bidirectional buck-boost converter for battery storage, and a cascaded Generalized Second-Order Integrator Phase-Locked Loop for accurate synchronization and reduced total harmonic distortion. Simulation results show the system can efficiently manage energy sharing among sources based on availability and load demand. During high renewable availability, the system minimizes reliance on the diesel generator, reducing fuel consumption and emissions. The battery system provides backup support during intermittent or low renewable generation, ensuring continuous power supply and stable operation. This work contributes to advancing hybrid microgrid technologies, offering a scalable and efficient solution for remote, off-grid, and urban microgrid applications.

Conflict of interest statement

Authors declare that they do not have any conflict of interest.

REFERENCES

[1] A. Qazi, F. Hussain, N. ABD. Rahim, G. Hardaker, D. Alghazzawi, K. Shaban and K. Haruna, "Towards sustainable energy: a systematic review of renewable energy sources, technologies, and public opinions," IEEE Access, vol. 7, pp. 63837-63851, 2019.

[2] B. Kroposki, B. Johnson, Y. Zhang, V. Gevorgian, P. Denholm, B. M. Hodge and B. Hannegan, "Achieving a 100% renewable grid: operating electric power systems with extremely high levels of variable renewable energy," IEEE Pow. Energy Mag., vol. 15, no. 2, pp. 61-73, March-April 2017.

[3] C. Cecati, C. Citro and P. Siano, "Combined operations of renewable energy systems and responsive demand in a smart grid," IEEE Trans. Sustain. Energy, vol. 2, no. 4, pp. 468-476, Oct. 2011.

[4] R. Billinton and R. Karki, "Maintaining supply reliability of small isolated power systems using renewable energy," IEE Proc. Gen. Trans. Dist., vol. 148, no. 6, pp. 530-534, Nov. 2001.

[5] F. Yang, X. Feng and Z. Li, "Advanced microgrid energy management system for future sustainable and resilient power grid," IEEE Trans. Ind. Appl., Early Access, 2019.

[6] A. Banerji, S. K. Biswas and B. Singh, "Enhancing quality of power to sensitive loads with microgrid," IEEE Trans. Ind. Appl., vol. 52, no. 1, pp. 360-368, Jan.-Feb. 2016.

[7] X. Liang, "Emerging power quality challenges due to integration of renewable energy sources," IEEE Trans. Ind. Appl., vol. 53, no. 2, pp. 855-866, March-April 2017.

[8] G. K. Taneja, G. Modi, B. Singh, and A. Verma, "Islanded solar PV-BESDG set for remote areas," in Proc. IEEE Uttar Pradesh Sect. Int. Conf. Elect., Electron. Comput. Eng., 2020, pp. 1–6.

[9] N. Ninad, D. Turcotte, and Y. Poissant, "Analysis of PV-diesel hybrid microgrids for small Canadian arctic communities," Can. J. Elect. Comput. Eng., vol. 43, no. 4, pp. 315–325, Oct. 2020.

[10] G. Shafiullah et al., "Prospects of hybrid renewable energy-based power system: A case study, post analysis of chipendeke micro-hydro, Zimbabwe," IEEE Access, vol. 9, pp. 73433–73452, 2021.

[11] T.-T. Ku and C.-S. Li, "Implementation of battery energy storage system for an island microgrid with high PV penetration," IEEE Trans. Ind. Appl., vol. 57, no. 4, pp. 3416–3424, Jul./Aug. 2021.

[12] A. Jahid, M. S. Islam, M. S. Hossain, M. E. Hossain, M. K. H. Monju, and M. F. Hossain, "Toward energy efficiency aware renewable energy management in green cellular networks with joint coordination," IEEE Access, vol. 7, pp. 75782–75797, 2019.

[13] N. Anglani, G. Oriti, and M. Colombini, "Optimized energy management system to reduce fuel consumption in remote military microgrids," IEEE Trans. Ind. Appl., vol. 53, no. 6, pp. 5777–5785, Nov./Dec. 2017.

[14] R.Manojkumar,C.Kumar, S.Ganguly, H. B. Gooi, S.Mekhilef, and J. P. S. Catalão, "Rule-based peak shaving using master-slave level optimization in a diesel generator supplied microgrid," IEEE Trans. Power Syst., early access, Jun. 29, 2022.

[15] R. Shi, X. Zhang, C. Hu, H. Xu, J. Gu, and W. Cao, "Self-tuning virtual synchronous generator control for improving frequency stability in autonomous photovoltaic-diesel microgrids," J. Modern Power Syst. Clean Energy, vol. 6, no. 3, pp. 482–494, May 2018.

[16] R. Sharma, S. Kewat, and B. Singh, "Power quality improvement in syrg-PV-BES-based standalone microgrid using ESOGI-FLL-WIF control algorithm," IEEE Trans. Ind. Appl., vol. 58, no. 1, pp. 686–696, Jan./Feb. 2022.

[17] K. Lai and M. S. Illindala, "Sizing and siting of distributed cloud energy storage systems for a shipboard power system," IEEE Trans. Ind. Appl., vol. 57, no. 3, pp. 1935–1944, May/Jun. 2021.

[18] K. Thirugnanam, S. G. Kerk, W. Tushar, and C. Yuen, "Energy management of islandedmicrogrid forreliability and cost trade-off with PV, energy storage, and diesel generator," IET Smart Grid, vol. 3, no. 6, pp. 870–881, Dec. 2020.

[19] S. Puchalapalli, S. K. Tiwari, B. Singh, and P. K. Goel, "A microgrid based on wind-driven DFIG, DG, and solar PV array for optimal fuel consumption," IEEE Trans. Ind. Appl., vol. 56, no. 5, pp. 4689–4699, Sep./Oct. 2020.

[20] C. Sun et al., "Design and real-time implementation of a centralized microgrid control system with rule-based dispatch and seamless transition function," IEEE Trans. Ind. Appl., vol. 56, no. 3, pp. 3168–3177, May/Jun. 2020.

[21] T. K.Roy,M.A. Mahmud, A.M.T. Oo,M.E.Haque,K.M.Muttaqi, andN. Mendis, "Nonlinear adaptive backstepping controller design for islanded DC microgrids," IEEE Trans. Ind. Appl., vol. 54, no. 3, pp. 2857–2873, May/Jun. 2018.

[22] V. Narayanan, S. Kewat, and B. Singh, "Control and implementation of a multifunctional solar PV-BES-DEGS based microgrid," IEEE Trans. Ind. Electron., vol. 68, no. 9, pp. 8241–8252, Sep. 2021.

[23] G. Modi and B. Singh, "Improved cascaded SOGI control for islandingsynchronization in photovoltaic system," IEEE Trans. Ind. Appl., vol. 58, no. 6, pp. 6909–6919, Nov./Dec. 2022.